Talanta 204 (2019) 525–532

Contents lists available at ScienceDirect

Talanta

journal homepage: www.elsevier.com/locate/talanta

Colorimetric multienzymatic smart sensors for hydrogen peroxide, glucose and catechol screening analysis

Oana Hosu[a,b], Mariagrazia Lettieri[a], Nicoleta Papara[a,b], Andrea Ravalli[a], Robert Sandulescu[b], Cecilia Cristea[b], Giovanna Marrazza[a,c,*]

[a] Department of Chemistry "Ugo Schiff", University of Florence, Via Della Lastruccia 3, 50019, Sesto Fiorentino (Fi), Italy
[b] Analytical Chemistry Department, Faculty of Pharmacy, "Iuliu Hatieganu" University of Medicine and Pharmacy, Pasteur 4, Cluj-Napoca, Romania
[c] Instituto Nazionale Biostrutture e Biosistemi (INBB), Unit of Florence, Viale Delle Medaglie D'Oro 305, 00136, Roma, Italy

ARTICLE INFO

Keywords:
Sensor
Colorimetric
Smartphone
Polyaniline
Polyanthranilic acid
Enzyme

ABSTRACT

In this work, we present a smartphone-based multiplexed enzymatic biosensor utilizing the unique colorimetric properties of the poly(aniline-*co*-anthranilic acid) (ANI-*co*-AA) composite film coupled with horseradish peroxidase (HRP), glucose oxidase (GOx), horseradish peroxidase-glucose oxidase (GOx-HRP) and tyrosinase (Tyr) enzymes. The enzymes are immobilized on the composite polymer film by adsorption and they catalyze a reversible redox color change of the host polymer from green to blue in the presence of their substrate. A smartphone was applied as color detector, for image acquisition and data handling. A ColorLab® android application, free of charge software application, was used to enable easy and clear display of the sensors' response indicating remarkable changes in the optical features. The results were confirmed by the spectrophotometric measurements. The developed colorimetric enzymatic biosensors were studied and optimized in relation to different experimental parameters. Moreover, the colorimetric enzymatic biosensors were applied to food and pharmaceutical analysis. It has been shown by these studies that the colorimetric biosensors are promising as quick and simple tests for handheld analysis in various fields.

1. Introduction

Disposable sensors represent a hot topic in the ongoing development of the biosensors due to their outstanding features including low price, simplicity and fast response, hence are highly preferred for replacing time–consuming centralized laboratory analysis. With billions of smartphones around the globe, which have become part of daily life, efforts have been devoted to the fabrication of mobile phone based devices [1,2]. In the last years, there is a here has been an exponential growth in the use of smartphones to improve health research and health care facilities [3]. In this context, there is also a great opportunity to expand the mobile technology to the bioanalytical sciences and many important advanced have been achieved [4]. Therefore, the incorporation of a mobile phone into a compatible detection platform represents a high throughout alternative among the nowadays approaches. In addition, utilizing its built-in sophisticated features, smartphone is often employed for the ability to autonomously collect, transmit, display and organize data for fast, real-time, and wireless point-of-care monitoring [1].

As a result, a wide applicability in biomedical related analysis was reported including DNA [5–7] and protein [8,9], drugs [10], gas [11], using colorimetric [12–14], electrochemical [15,16], fluorescent [17], and luminescent [10,18] approaches. Some of them are integrated with sensors, such as test strips, multi-well plates, microchips, and hand-held detectors for applications in healthcare diagnosis, environment monitoring, and food evaluation [1,2,19]. In the case of multi-well plates, the smartphone features are expected to replace the microplate reader as an integration of more portable and much more cost-effective instrumentation [20]. However, challenges such as optical aberrations must be overcame as influences the overall analytical performance of the sensor. Some studies have been reported for optimizing the illumination during the smartphone-based analysis [21]. Hence, microprism or optical fiber arrays were employed to solve these problems [22], but thus the sensor development lacks of simplicity. When enlarging the shooting distance [23] and capturing the "before" and "after" images of the array in the same experimental conditions, the picture can be taken at a suitable distance without optical aberrations.

Some smartphone-based devices are commercial available for point of care testing of various analytes using sweat, saliva and blood [24]; as the devices are obtained by complex microfluidic and wax printing

* Corresponding author. Department of Chemistry "Ugo Schiff", University of Florence, Via della Lastruccia 3, 50019, Sesto Fiorentino (Fi), Italy.
E-mail address: giovanna.marrazza@unifi.it (G. Marrazza).

https://doi.org/10.1016/j.talanta.2019.06.041
Received 28 February 2019; Received in revised form 6 June 2019; Accepted 10 June 2019
Available online 12 June 2019
0039-9140/

techniques and costly reagents, the cost for each analysis is expansive. Here, we present a multiplexed enzymatic strip more cheaply and friendly to prepare for hydrogen peroxide, glucose and catechol detections.

Different optical signalers of the multi-well arrays have been reported *i.e.* gold and silver nanoparticles [25,26], ELISA substrates [27,28], or polymers [29,30]. Polyaniline (PANI) is an extensively investigated polymer and has intrigued the scientific community due to its concomitant chemical, electrical and optical properties [31,32]. The emeraldine salt form is a very attractive polymer for electrical conductivity, mechanical flexibility, easy of synthesis, environment stability and redox properties [33–37]. Moreover, it has the ability to change the optical properties that can be reversible through redox and protonation-deprotonation reactions [38]. However, its insolubility in common solvents, which results in difficult process abilities, has restricted its applications. To improve the polymer solubility, co-polymerization of aniline with aniline derivatives was proposed [39]. On co-polymerization of aniline with *o*-anthranilic acid there is the formation of a material having better electro-properties than their homopolymers.

Polyanthranilic acid, a carboxylated aniline based polymer capable of self-doping, is of interest as a soluble derivative of polyaniline [40,41].

The achievement of multiplexed colorimetric enzymatic biosensors for three model enzymes, namely hydrogen peroxidase (HRP), glucose oxidase (GOx), and tyrosinase (Tyr), based on poly(aniline-*co*-anthranilic acid) composite polymer and mediated by a smartphone camera readout, is reported. The co-polymer of aniline and anthranilic acid was synthesized by chemical route on both polyester microplates and strips and was further used for the immobilization of the enzymes by adsorption. The spontaneous redox reaction of poly(ANI-*co*-AA) via the enzymatic reaction and the consumption of the substrate (hydrogen peroxide, glucose and catechol, respectively) results in a color change from green to blue. Therefore, the enzymatic reaction can be optically monitored.

Since glucose and polyphenol determination plays an important role in clinical and environmental fields [42–45]. The glucose monitoring is a valuable tool for the management of diabetes patients. Diabetes is a worldwide disease that affects hundreds of millions of people. Fortunately, with a careful diet and appropriate medications, the complications of diabetes can be greatly reduced. These treatments involve the continuous monitoring of blood glucose levels so that they can intervene promptly if they become too high. The concentration range of glucose in clinical samples is 5–30 mM. Moreover, the glucose measurement is also useful in food analysis. Food samples (fruit juices, soft and energy supplying drinks etc.) generally have higher glucose concentrations than clinical samples around 500 mM. Therefore, the application of an extended linearity biosensor is necessary. During the last decade, glucose biosensor technology including point-of-care devices has made glucose measurement fast, easy and inexpensive. However, there are continuous advances in research related to the achievement of accurate and reliable glucose monitoring.

Phenolic contaminants are known as major effluents produced by various chemical and metal processing industries and cause severe pollution of groundwater. They have been recognized as toxic substances and endocrine disruptors. For these reason, the determination of phenolic compounds in environmental matrices, including tap and surface water, has become a matter of great concern and scientific interest. Furthermore, phenols present in vegetables and fruit (grapes and grape skins) and in many derivatives, such as wine, olive oil, coffee and tea, are powerful antioxidants, against low density lipoproteins, rich in cholesterol, carrying out an important protective action on our arteries, in the prevention of atherosclerosis and cardiovascular diseases. Therefore, the monitoring of catechol concentration, in micromolar range, as indicator of phenolic compounds becomes of fundamental importance for the safety of the environment and for food quality.

Here, we present a colorimetric multiplexed platform applied for their direct determination from different food and pharmaceutical samples. It was demonstrated, not only the enhanced optical signals given by the enzymatic reaction at the poly(ANI-*co*-AA) composite film, but moreover the assisted film formation that serves as matrices for the enzyme immobilization. The achievement of a single use and disposable colorimetric biosensor has several advantages due to its low cost, mass production, simplicity and portability. This new approach can be a useful tool for practical analytical applications in screening tests involving polyphenol and glucose determination and could be extended for future handheld configurations.

2. Material and methods

2.1. Chemicals

Aniline (ANI), anthranilic acid (AA), tyrosinase (Tyr) from mushrooms (Type II; 2085 U/mg), horseradish peroxidase (HRP) (Type II; 210 U/mg), glucose oxidase (GOx) from Aspergillus niger, (Type II-S; 26820/g), *N*-hydroxysuccinimide (NHS), 1-ethyl-3-(3-dimethylaminopropyl) carbodiimide (EDC), catechol, hydrogen peroxide solution (30% w/w), D(+)glucose, mannitol, maltose, fructose, ascorbic acid, aspartic acid, uric acid, sodium peroxodisulfate and 96-wells microplates were purchased from Sigma Aldrich (Italy, www.sigmaaldrich.com). Sodium chloride, sodium acetate trihydrate, nitric acid and hydrochloric acid were purchased from Merck (Italy, www.merck.com).

All chemicals were of analytical reagent grade and were used as received without any further purification. All solutions were prepared using water obtained from Milli-Q Water Purification System (resistivity ≥ 18 MΩ cm) (Germany, www.merckmillipore.com). Polyester film was obtained from MacDermide (Italy, www.autotype.macdermid.com).

2.2. Instrumentation

iMark™ Microplate Absorbance Reader was purchased from Biorad (Milan, Italy, www.bio-rad.com). Scanning electron microscopy (SEM) analysis was carried out using Gaia 3, Tescan (Czech Republic, www.tescan.com). Infrared measurements were performed using IR Shimadzu Scanning spectrometer (model 8400S) in the range 600–4000 cm^{-1} with an ATR module (diamond prism supported by a ZnSe lens) and a resolution of 4 cm^{-1} (Japan, www.shimadzu.com).

The images were acquired with an android smartphone (equipped with 16 megapixel camera) and analyzed by ColorLab® Google Play Store android application (www.play.google.com). The data were processed using Origin 8 pro software (OriginLab, Northampton USA, www.originlab.com).

2.3. Multiplexed colorimetric enzymatic biosensors protocol

2.3.1. Preparation of poly(ANI-co-AA) composite film

The co-polymerization of aniline and anthranilic acid was firstly performed onto 96-well micro-plates by chemical oxidation mixing 900 µL of 100 mM aniline solution with 100 µL of 50 mM anthranilic acid solution in 1.0 M HCl. 50 µL of this solution was mixed with 50 µL of 100 mM sodium peroxodisulfate solution in 1.0 M HCl. After that, 100 µL of this solution was dropped using a micropipette in each well of the microplate. The polymerization was allowed to proceed overnight (≈16 h) at 4 °C. During this period, the microplate was covered to avoid any evaporation of the solution. Then, the wells were washed three times with distilled water to remove the unreacted solution.

To realize co-polymer modified strips, a polyester substrate was cut into 2 × 6 cm size sheets and immersed in the polymerizing solution in the experimental conditions as previously described. The overload polymerizing solution adhering on the surface of the substrate was removed by washing with Mili-Q water. The modified strip was stored under dry condition at room temperature for further use. For all the

experiments, square-shaped sensing elements with dimension of $1 \times 1\ cm^2$ were prepared by cutting the larger sensor substrate.

The co-polymer modified surface was characterized by scanning electron microscopy.

2.3.2. Enzymatic biosensors

The co-polymer modified surfaces were used as platform for HRP, GOx, GOx-HRP and Tyr enzyme color sensors. 100 µL of each enzyme solution in 0.1 M PB pH 5.0 were dropped on the co-polymer modified wells and left to incubate overnight (≈16 h) at 4 °C. In particular, we used for the realization of hydrogen peroxidase and glucose biosensor 12.5 U/mL of HRP or of GOx, for GOx-HRP bi-enzymatic approach 12.5 U/mL of each and 40 U/mL of Tyr in the case of tyrosinase.

In order to realize the enzymatic strips, the co-polymer modified strips were immersed in the enzymatic solutions at the same concentration used for the wells and left to incubate overnight at 4 °C. The solutions were then discarded; the wells and the strips were washed thoroughly three times with PB pH 5.0.

The modified enzyme/poly(ANI-*co*-AA) composite platforms were then stored in dry conditions at 4 °C prior to use in order to preserve the enzymatic activity.

2.3.3. Biosensor measurements

Various concentrations of the analytes (hydrogen peroxide, glucose and catechol) were prepared in 0.1 M PB pH 5.0 and a volume of 100 µL was directly dropped on the biosensor wells or 200 µL on the biosensor strips for 2 min for each hydrogen peroxide and catechol substrates, and 8 min in the case of glucose. The sample solutions were then removed and the color change was measured by Microplate Absorbance Reader or smartphone camera as the measurable response of the biosensor toward analyte quantification.

The control experiments were performed in the same procedure using the co-polymer film in a solution free of analyte (S_0) as well as the response of the sensor with no enzyme (S_0`). Therefore, the signal is attributed by subtracting the value of the analyte generated colored wells or strips with that of the blank.

In order to study the non-specific response of the biosensors, experiments were performed using solutions of mannitol (Man), maltose (Mal), fructose (Fru), ascorbic acid (Asc), aspartic acid (Asp), and uric acid (Ua).

The biosensor wells and strips were used for single-use. Each analysis was repeated at least 5 times using various enzymatic biosensors.

2.4. Data and quantitative image processing

Although the color change can be easily examined by naked eye during the analyte detection, after the reaction took place, an android-based smartphone was used as color detector, for image acquisition and data handling for quantitative analyses. A ColorLab® android application, free of charge software application, was used to enable easy and clear display of the sensors' response indicating remarkable changes in the optical features. The average green and blue values of the enzyme modified wells and strips were automatically calculated by the application via the “Eye dropper” feature, which provides different parameters that could be assessed from the image. The HSV (Hue, Saturation, and Value) data is a cylindrical coordinate, which correspond to the color appearance parameters described by: Hue (H), Saturation (S) and Value (V) [40,46]. The model was explained in detail in a previous work [14]. Hue was found to be more suitable in retrieving a direct correlation between the analyte concentration and the color change as the wells were turning from green to blue with increased concentration of the analyte. The smartphone images were captured at a fixed distance (60 mm) from the gadget's screen to prevent the parallax error and with the flashlight of the smartphone of obtaining response in order to minimize ambient light interferences that may result in false readings. The image-processing algorithm initially determines the center of each color spot to calculate the mean pixel intensity of 20 neighboring pixels. ColorLab® android application converted the pixel intensity of acquired images by an image processing algorithm. The ΔHue values calculated as ($Hue_{conc.}$–Hue_{Blank}) is then plotted against the analyte concentration.

The results were confirmed by the spectrophotometric measurements using a Microplate Absorbance Reader at 655 nm.

2.5. Sample analysis

Preliminary experiments for the determination of target analytes in commercially available samples were also performed. All real samples were first filtered (0.45 µm) and diluted (1:200) in 0.1 M PB pH 5.0 for further standard additions of the analytes. The samples analyzed were: red and white wine, pear juice, pomegranate fresh juice, pharmaceutical formulation consisted of sachets of 15 g (D-Mannitol, *Vaccinium macrocarpum* - cranberry) which were dissolved in 50 mL Milli-Q distilled water. The biosensor response was then determined by colorimetric measurements under the same conditions used for the calibration plots.

3. Results and discussion

The main objective of this work was to design multiplexed colorimetric enzymatic biosensors coupled with smartphone as transducer for screening analysis. The colorimetric biosensor were studied and optimized with respect to several experimental parameters in order to find the best conditions for the sample analysis. The protocol involves in the following steps: a) aniline and anthranilic acid chemically co-polymerization on the polyester substrate; b) enzymes immobilization; c)

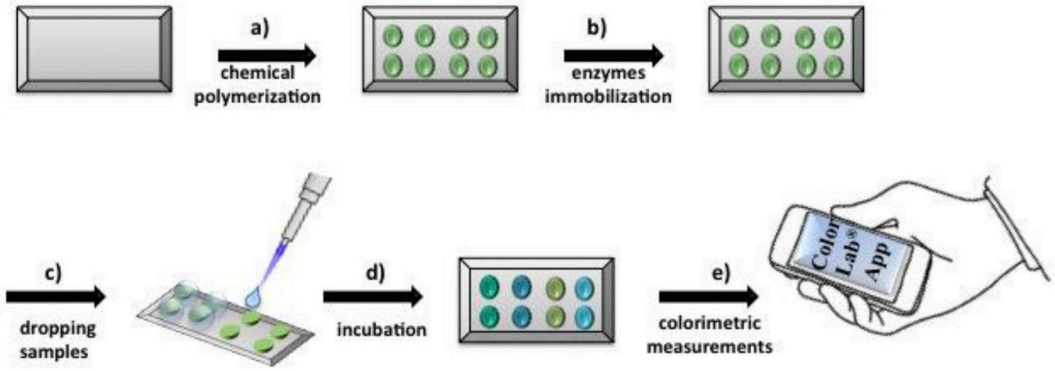

Fig. 1. Scheme of the multiplexed enzymatic assay: a) aniline and anthranilic acid chemically co-polymerized on the polyester substrate; b) enzymes immobilization by spotting the solutions onto the substrate; b) incubation with samples; c) capture of the colorimetric change using the smartphone's camera and evaluation of data handling via a specific application.

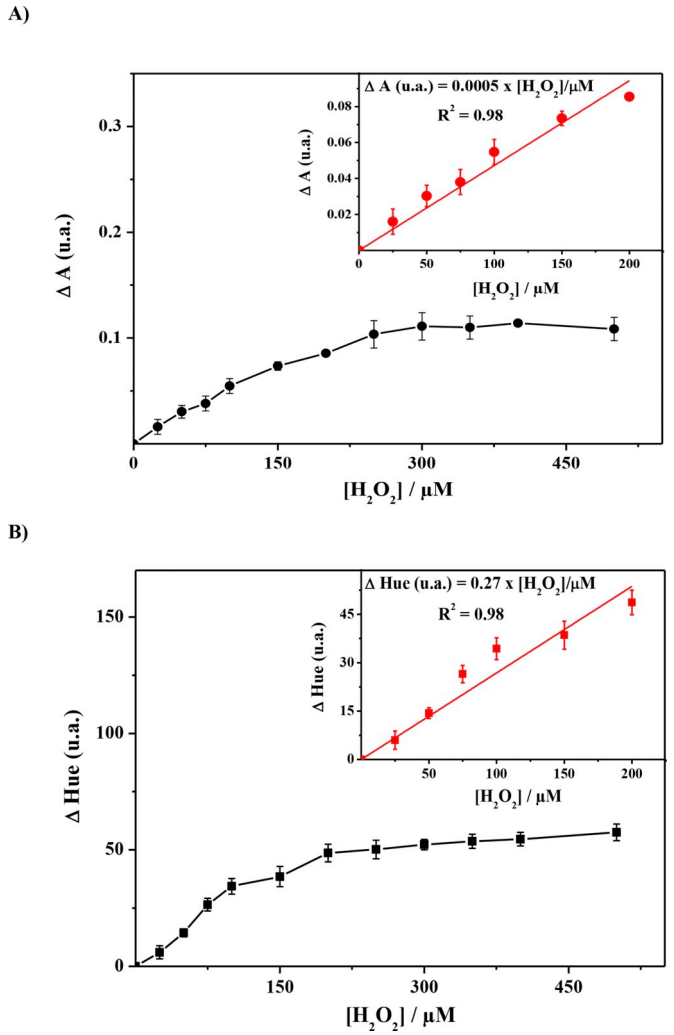

Fig. 2. Response of the HRP/poly(ANI-*co*-AA) sensor (S_1–S_0) in the presence of hydrogen peroxide solutions in 0.1 M PB pH 5.0 analyzed by A) Microplate Absorbance Reader at 655 nm (●); B) ColorLab® smartphone application (■); inset: corresponding calibration plots. Each point was repeated at least 5 times using various hydrogen peroxidase biosensors.

spotting sample solutions; d) incubation with samples; e) capture of the colorimetric change using the smartphone's camera and f) evaluation of data handling via a specific application (Fig. 1). The smartphone-based microplate and strips approaches are shown in Fig. 1S.

3.1. Co-polymer spectroscopic and microscopic characterization

Aniline and anthranilic acid were chemically co-polymerized using sodium peroxodisulfate as oxidant onto the microplate wells and the strips as described in the Materials and Methods section. The most plausible structure of the co-polymer is shown in Fig. S2 A.

Firstly, the aniline and anthranilic acid co-polymerization was studied by ATR-IR spectroscopy. The representative spectrum of poly(ANI-*co*-AA) is shown in Fig. S2 B in the frequency range from 600 to 4000 cm^{-1}. PANI is characterized by the presence of a characteristic peak at 3414.00 cm^{-1} assigned to the stretching N–H bond. The peak at 2841.15 cm^{-1} is due to the C–H stretching vibration. The peak at 1481.47 cm^{-1} is attributed to N = Q = N stretching [47]. The absorption peaks at 819.88 (C–H), 1109.07 (C–N), and 1303.88 (C–H) cm^{-1}, are assigned to C–H bending vibration out of plane, stretching vibration of C–N bond, and C–H bending, respectively [48]. The peaks at 1564.27 and 1637.55 cm^{-1} are due to C=O stretching of carboxylic acids.

Fig. S2 B shows the ATR-IR spectra of the presence of C=O, C–O and OH in the spectra of PANI which demonstrates the successfully co-polymerization of the aniline with anthranilic acid.

Moreover, SEM technique was used to verify the aniline and anthranilic acid chemical co-polymerization. SEM images are shown in Fig. S2: C) unmodified polyester substrate; D) poly(ANI-*co*-AA) modified polyester substrate in optimized experimental conditions. It is possible to observe that the film obtained is uniform on the substrate, therefore showing its possible use as a rapid colorimetric assay.

3.2. Enzymatic assays

3.2.1. Hydrogen peroxidase biosensor

The HRP biosensor was optimized with respect to several experimental conditions such as enzyme immobilization, pH buffer and substrate incubation time.

In order to find the optimal amount of enzyme immobilized and the incubation time with substrate, poly(ANI-*co*-AA) sensors were modified with 5 U/mL, 12.5 U/mL and 25 U/mL enzyme solutions, prepared in 0.1 M PB buffer pH 5.0, and incubated at 2, 5 and 8 min with the H_2O_2. It was observed that this reaction depends not only on the concentration of hydrogen peroxide and enzyme activity, but also on the reaction time, and can induce dramatic changes in optical properties that are visible by the naked eye. Therefore, the substrate was left to react as the color was changing from green to blue in accordance with the substrate concentration. For this purpose, the experimental parameters were chosen taking into consideration the Absorbance signal difference ($\Delta Abs = Abs_{S_1} - Abs_{S_0}$) between 100 μM ($Abs_{S_1}$) and 0 μM H_2O_2 (Abs_{S_0}) and the best reproducibility in terms of % Relative Standard Deviations (% RSD) (n = 5) measured by spectrophotometric analysis. The results showed that 12.5 U/mL of HRP and 2 min of analyte incubation time ensured an optimum of the colorimetric response which were then selected for further experiments (data not shown).

To assess the influence of the pH variation, the efficiency of the HRP/poly(ANI-*co*-AA) sensor was tested with hydrogen peroxide solutions prepared in 0.1 M PB in the pH range from 5.0 to 8.0. The best results both in terms of sensitivity and reproducibility were obtained at pH 5.0 measured by spectrophotometric analysis (Fig. S3).

A biosensor response at optimized parameters was obtained in presence of H_2O_2 in the concentration range from 25 to 500 μM. A linear correlation in the range 25–200 μM H_2O_2 with a limit of detection (LOD = $3S_{blank}$/Slope [49]), of 35.6 μM by spectrophotometric analysis and 51.2 μM by ColorLab® smartphone application were obtained (Fig. 2 A, B).

3.2.2. Glucose oxidase biosensor

In order to realize the glucose biosensor, 12.5 U/mL GOx solution prepared in 0.1 M PB buffer pH 5.0 was dropped on the co-polymer film for overnight physical adsorption. After washing with PB, the biosensor was further incubated for 2 min in glucose solution concentration ranging from 25 to 500 μM. The biosensor response was tested in 0.1 M PB in the pH range from 5.0 to 8.0. The better response was obtained at pH 5.0 measured by spectrophotometric analysis (data not shown). Thus, 0.1 M PB pH 5.0 buffer was selected for further experiments.

A linear range was achieved in the 25–200 μM range with LODs of 95 μM by spectrophotometric analysis and 109 μM by ColorLab® smartphone application, respectively (Fig. 3 A, B).

In order to increase the sensitivity of the glucose biosensor, for the following experiments, GOx-HRP bi-enzymatic system was applied. Both enzymes systems were co-immobilized at the polymeric modified wells in an equal ratio (12.5 U/mL). The color change was due to the enzymatic product with co-polymer interaction. The optimal reaction time in the case of the bi-enzymatic system was found to be higher (8 min) than HRP/poly(ANI-*co*-AA) alone (2 min). This effect could be probably due to a higher total enzyme concentration compared to HRP

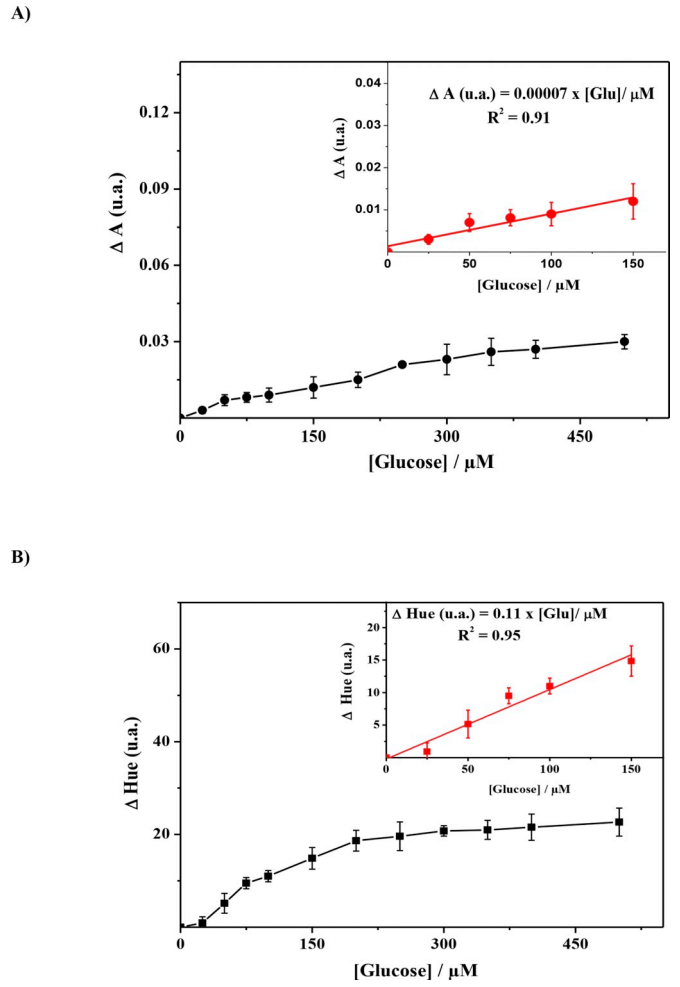

Fig. 3. Response of the GOx/poly(ANI-*co*-AA) sensor (S_1–S_0) in the presence of glucose in 0.1 M PB pH 5.0 analyzed by A) Microplate Absorbance Reader at 655 nm (●); B) ColorLab® smartphone application (■); inset: corresponding calibration plots. Each point was repeated at least 5 times using various glucose biosensors.

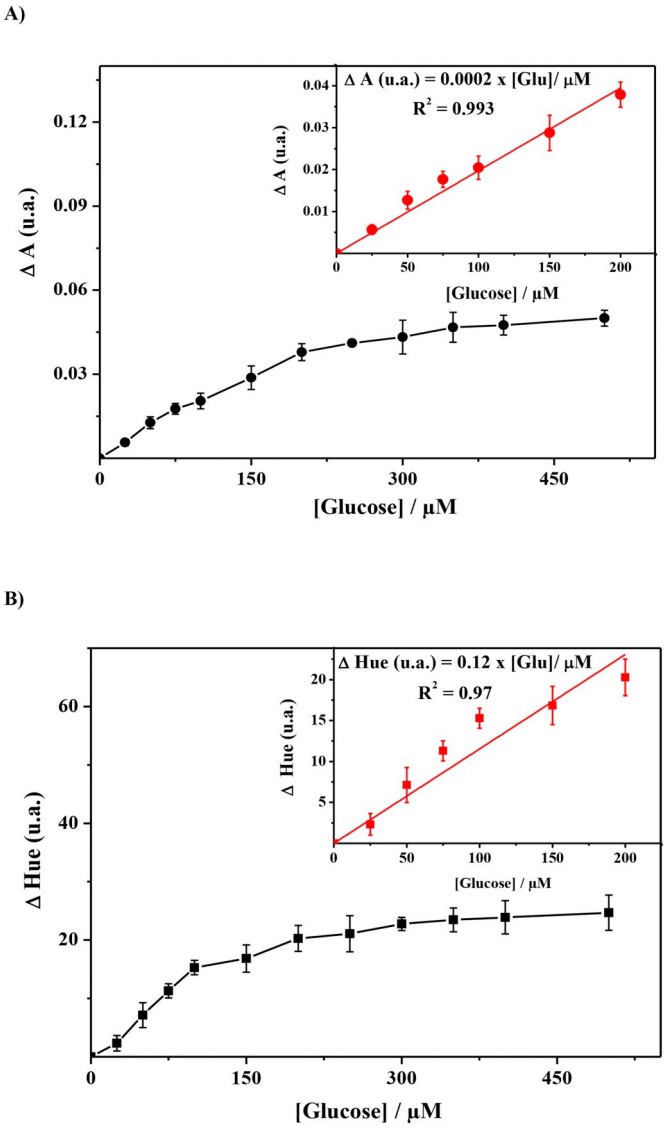

Fig. 4. Response of the GOx-HRP/poly(ANI-*co*-AA) sensor (S_1–S_0) in the presence of glucose in 0.1 M PB pH 5.0 analyzed by A) Microplate Absorbance Reader at 655 nm (●); B) ColorLab® smartphone application (■); inset: corresponding calibration plots. Each point was repeated at least 5 times using different glucose biosensors.

alone as well as the steric hindrance in the protons speed exchange involved in the polyaniline color change. Upon exposure to glucose solution, the sensors show two calibration curves in the range of 25–200 μM. The equations obtained by both spectrophotometric and smartphone application analysis are described below: ΔA (u.a.) = 0.0002 × [Glu] (μM); R^2 = 0.993; ΔHue (u.a.) = 0.12 × [Glu] (μM); R^2 = 0.97. The LODs were 27.7 μM by spectrophotometric analysis and 49.4 μM by ColorLab® smartphone application, respectively (Fig. 4 A, B).

For an analytical chemistry application where the selectivity of the sensing system is crucial, the as-prepared bi-enzymatic assay (GOx-HRP)/poly(ANI-*co*-AA) colorimetric response was evaluated in the presence of different interfering substances including mannitol (Man), maltose (Mal), fructose (Fru), ascorbic acid (Asc), aspartic acid (Asp), and uric acid (Ua). Two different concentrations were used: (i) 200 μM, which is the upper limit from the glucose calibration plot and (ii) 5-fold more concentrated solution, in order to prove the specificity of the biosensor. The color modification was assessed by both spectrophotometric and smartphone readout. As can be seen from Fig. S4, the ΔHue ($Hue S_1$ – $Hue S_0$) value of Man, Mal, Fru, Asp and Ua remain the same for both concentrations with a maximum % RSD of 4.2. By increasing the glucose concentration, a remarkable blue shift in the Vis spectra corresponding to the emeraldine base enzymatic generated conversion was observed. In the case of ascorbic acid (Asc), it was found a visual color change from green to light yellow which corresponds to the leucoemeraldine form of the undoped polyaniline [50]. The % RSD obtained for Asc in terms of ΔHue value at the modified GOx-HRP/poly(ANI-*co*-AA) for both concentrations was lower than 10%. This demonstrates that the colorimetric sensor possesses high sensitivity and can be employed for practical applications.

3.2.3. *Tyrosinase biosensor*

The optimal concentration for the Tyr/co-polymer composite film was found to be 40 U/mL for overnight reaction onto the polymer modified substrate. For 12.5 U/mL enzyme concentrations little change for different catechol concentrations was obtained, whereas for 100 U/mL tyrosinase the wells color were changing to dark blue in the first 30 s. Therefore, an intermediate enzyme concentration solution (40 U/mL) was tested and used for further experiments. The biosensor response was tested in 0.1 M PB in the pH range from 5.0 to 8.0. The best results were obtained at pH 5.0 measured by spectrophotometric analysis (data not shown). Thus, 0.1 M PB pH 5.0 buffer was chosen for further experiments. The modified substrate was washed three times

with PB pH 5.0 buffer solution and subsequently the sensor was tested in the presence of different concentrations of catechol ranging from 2.5 to 200 µM in 0.1 M PB pH 5.0 at room temperature. The optimal reaction time was found to be 2 min, since the ΔAbs ($AbsS_1$-$AbsS_0$) was two times higher than that of 1 min, whereas for 3 min reaction time the increase in the absorbance value was only of 13%. The data were compared taking into account the absorbance values of 10 µM catechol and 0 µM catechol in 0.1 M PB pH 5.0. Therefore, 2 min was chosen for further experiments.

It can be seen from Fig. S5 that the HSV coordinates are automatically calculated by the "Eye Dropper" feature of the ColorLab® smartphone application just by pointing the cursor in the specific well from the microplate. With camera readout, a trade-off between the ease of use and limit of detection was expected. Therefore, the limit of detection was compared using smartphone based-visual determination with absorbance spectroscopy.

By subtracting the absorbance ($AbsS_0$) and Hue ($HueS_0$) value of the blank from the signal of the catechol generated colored wells, two calibration plots (2.5–50 µM catechol) were obtained with the following equations: ΔA (u.a.) = 0.001 × [Catechol] (µM), R^2 = 0.98; ΔHue (u.a.) = 0.78 × [Catechol] (µM), R^2 = 0.96, respectively (Fig. 5 A, B). Although in the case of catechol, a slightly lower limit of detection (LOD) of 12.3 µM, was obtained in the case of smartphone analysis, by spectrophotometric analysis a LOD of 16.2 µM was determined. The µM limit of detection for catechol is promising as colorimetric detection offers an equipment-free method of analysis.

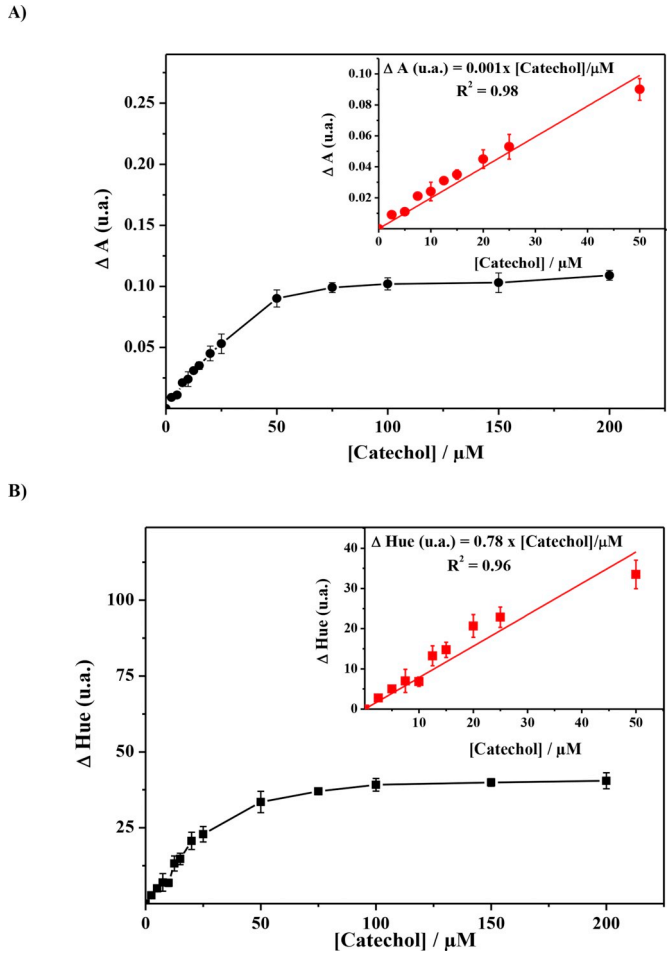

Fig. 5. Response of the Tyr/poly(ANI-*co*-AA) sensor (S_1–S_0) in the presence of catechol in 0.1 M PB pH 5.0 analyzed by A) Microplate Absorbance Reader at 655 nm (●); B) ColorLab® smartphone application (■); inset: corresponding calibration plots. Each point was repeated at least 5 times using various tyrosinase biosensors.

3.3. Reproducibility and stability of multienzymatic biosensors

In order to test the reproducibility of the proposed biosensor, at least 5 determinations on different biosensors were assayed for each concentration and the average % RSD was calculated. The results show good reproducibility with 8% intra-coefficient of variation.

The enzyme-modified co-polymer assay showed good operational stability maintaining 95% of the initial response after 1 month of storage in dry condition at 4 °C. Moreover, 36 strips were stored in a thermostatic oven at 37 °C for one month. Three strips of each enzyme biosensor were measured every week incubating with 100 µM of glucose and H_2O_2 solutions and with 5 µM catechol solution. The ΔHue value after four weeks was decreased of around 6% for glucose biosensor, 4% for H_2O_2 biosensor and 8% for catechol biosensor with respect to the first measurement. This confirms that the enzymatic biosensors have a good stability. It can be attributed to the excellent biocompatibility of the enzymatic system with the co-polymer network.

The results confirm good analytical performance of the proposed colorimetric sensors related to the good entrapment of the enzymes at the poly(ANI-*co*-AA) sites on the multi-well and polyester substrates which greatly boost the colorimetric response of the robust network system.

3.4. Enzymatic strips

To test the performance of the detecting enzymatic biosensors realized in strip format, experiments were carried out with HRP/poly(ANI-*co*-AA), GOx-HRP/poly(ANI-*co*-AA) and Tyr/poly(ANI-*co*-AA) modified strips. A significant change color was observed. The depths of the color changes were analyzed and normalized using image processing resulting in quantificable concentration measurements. Calibration plots for hydrogen peroxidase, glucose and cathecol was reported in Fig. 6. The obtained LODs were 11 µM for hydrogen peroxide, 20 µM for glucose and 2.4 µM for catechol, respectively.

3.5. Real sample analysis

The as-prepared biosensors were tested for catechol and glucose determination in several commercially available samples: red and white wine, pear juice, pomegranate fresh juice and pharmaceutical product. The determinations were made using the standard addition method and results are displayed in Table 1. The color modification was assessed by the two analytical methods. Although, by the presence of the reducing agents in the real samples (*i.e.* ascorbic acid) the part of the blue emeraldine base form of the polyaniline can be converted to the reduced form of yellow leucomeraldine [50,51]. Therefore, a supplementary subtraction of the signal obtained at the unmodified co-polymer matrix in the presence of the real sample (S_0`) was performed. Hence, the ΔAbs and ΔHue were directly related to the enzymatic conversion of the substrate retrieved in the sample by the standard addition method. Moreover, by the 1:200 dilution step of the samples, interference reactions were avoided, as the enzymatically reaction of the substrates is specific for threshold analyte concentration. For catechol determination, the recovery factors between the two methods were relatively close to 100%, showing that there were no significant interferences from the other compounds present in the samples. These results reveal that as-prepared smart biosensors can be effectively used for sensing applications of glucose and catechol (polyphenol) in foods and pharmaceutical formulations and potentially in biological fluids.

4. Conclusion

This concept showed a vivid colorimetric response from light green to dark blue specifically to three analytes named hydrogen peroxide,

A)

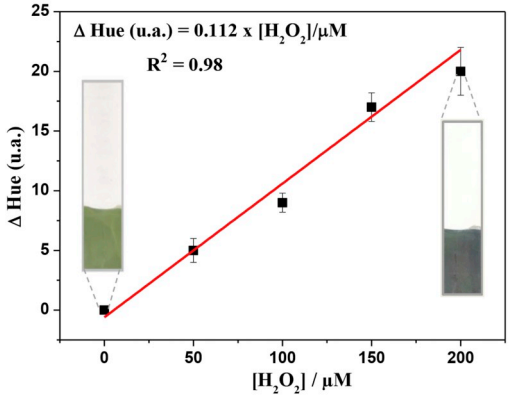

B)

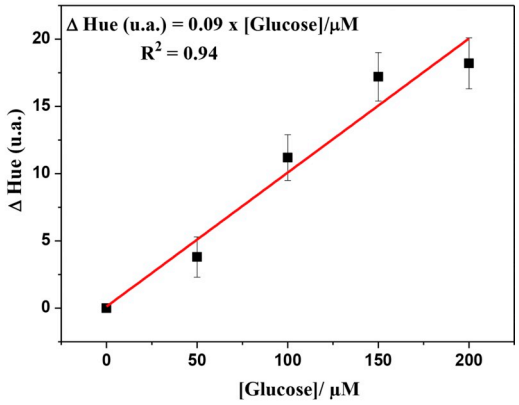

C)

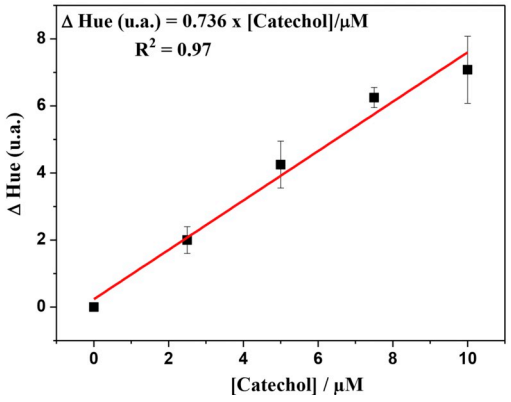

Fig. 6. Calibration plots analyzed by ColorLab® smartphone application: A) HRP/poly(ANI-*co*-AA) sensor; B) GOx-HRP/poly(ANI-*co*-AA) sensor and C) Tyr/poly(ANI-*co*-AA) sensor realized by enzymatic strips. Each point was repeated at least 5 times using various biosensors strips.

glucose and catechol. Additionally, the sensing responses were visualized by employing two analysis methods that translates measured UV spectra and camera smartphone readout into numeric color values directly related to analyte concentration and therefore to color perception. The biosensor has been shown to exhibit good sensitivities as μM levels of catechol were detected visually within 2 min. In addition, the biosensor was tested in the presence of hydrogen peroxide by using the HRP-modified co-polymer system or coupled with GOx enzyme for glucose detection. Finally, the trade-off between the easy of use and limit of detection was quantified by analyzing the data obtained by smartphone readout compared to spectrophotometric ones. In the case of catechol, the LOD was 14 ± 2 μM for both techniques, whereas in the case of hydrogen peroxide and glucose the LOD improved by less than using the ColorLab® smartphone-based analysis. Real sample analysis was performed for catechol and glucose determination and good recovery factors were obtained. According to the results here reported, the fabricated strips presented satisfactory analytical performance. The reproducibility achieved for the realized platforms were acceptable taking into consideration that all the fabrication steps are handmade. Moreover, enzymatic biosensors realized in strip format provide not only a promising analytical method for the label-free detection of hydrogen peroxide glucose and catechol but also an easy and an attractive route for the further fabrication of smart biosensors with many potential applications for screening tests. Therefore, the platforms developed for the point of use quantification of multiple analytes represents an innovative approach to reduce time, cost and sample volumes. As the fabrication process is quite simple and the materials used are inexpensive, the platforms proposed in this work, after further optimization, could be successful marketed.

Table 1
Real sample analysis using the enzyme-based poly(ANI-*co*-AA) sensor by microplate Absorbance Reader at 655 nm and ColorLab® smartphone application. Each analysis was repeated at least 5 times using different sensors.

Enzyme	Sample	Elisa reader (655 nm) (mM)	Smartphone App (mM)	Recovery* (%)
GOx + HRP	a	2.36	2.05	87
	b1	3.13	3.34	107
	b2	0.68	0.73	107.
	c	1.90	1.74	91
	d	1.96	1.99	101
Tyr	a	0.49	0.43	87
	b1	1.15	1.21	105
	b2	1.58	1.52	96
	c	0.45	0.47	104
	d	0.36	0.39	108

a – Pharmaceutical sample, b – Fruit juice (b1 - pear juice, b2 - pomegranate fresh juice); c – Red wine; d – White wine.

Acknowledgements

This work was supported by a grant of the Romanian National Authority for Scientific Research and Innovation, CCCDI – UEFISCDI, project number PN–III–P1-1.2-PCCDI2017-0407.

Appendix A. Supplementary data

Supplementary data to this article can be found online at https://doi.org/10.1016/j.talanta.2019.06.041.

References

[1] H. Xu, L. Cheng, C. Wang, X. Ma, Y. Li, Z. Liu, Polymer encapsulated upconversion nanoparticle/iron oxide nanocomposites for multimodal imaging and magnetic targeted drug delivery, Biomaterials 32 (2011) 9364–9373, https://doi.org/10.1016/j.biomaterials.2011.08.053.
[2] D. Zhang, Q. Liu, Biosensors and bioelectronics on smartphone for portable biochemical detection, Biosens. Bioelectron. 75 (2016) 273–284, https://doi.org/10.1016/j.bios.2015.08.037.
[3] S.K. Vashist, P.B. Luppa, L.Y. Yeo, A. Ozcan, J.H.T. Luong, Emerging technologies for next-generation point-of-care testing, Trends Biotechnol. 33 (2015) 692–705, https://doi.org/10.1016/J.TIBTECH.2015.09.001.
[4] S.K. Vashist, O. Mudanyali, E.M. Schneider, R. Zengerle, A. Ozcan, Cellphone-based devices for bioanalytical sciences multiplex platforms in diagnostics and bioanalytics, Anal. Bioanal. Chem. 406 (2014) 3263–3277, https://doi.org/10.1007/

s00216-013-7473-1.
[5] H. Ilkhani, S. Farhad, A novel electrochemical DNA biosensor for Ebola virus detection, Anal. Biochem. 557 (2018) 151–155, https://doi.org/10.1016/j.ab.2018.06.010.
[6] H. Subak, D. Ozkan-Ariksoysal, Label-free electrochemical biosensor for the detection of Influenza genes and the solution of guanine-based displaying problem of DNA hybridization, Sensor. Actuator. B Chem. 263 (2018) 196–207, https://doi.org/10.1016/j.snb.2018.02.089.
[7] E. Eksin, A. Erdem, Electrochemical detection of microRNAs by graphene oxide modified disposable graphite electrodes, J. Electroanal. Chem. 810 (2018) 232–238, https://doi.org/10.1016/j.jelechem.2018.01.015.
[8] J. Zhou, Y. Yang, C. Zhang, Toward biocompatible semiconductor quantum dots: from biosynthesis and bioconjugation to biomedical application, Chem. Rev. 115 (2015) 11669–11717, https://doi.org/10.1021/acs.chemrev.5b00049.
[9] M. Braiek, M.A. Djebbi, J.F. Chateaux, A. Bonhomme, R. Vargiolu, F. Bessueille, N. Jaffrezic-Renault, A conductometric creatinine biosensor prepared through contact printing of polyvinyl alcohol/polyethyleneimine based enzymatic membrane, Microelectron. Eng. 187–188 (2018) 43–49, https://doi.org/10.1016/j.mee.2017.11.018.
[10] R. Griss, A. Schena, L. Reymond, L. Patiny, D. Werner, C.E. Tinberg, D. Baker, K. Johnsson, Bioluminescent sensor proteins for point-of-care therapeutic drug monitoring, Nat. Chem. Biol. 10 (2014) 598–603, https://doi.org/10.1038/nchembio.1554.
[11] G. Shi, Y. He, Q. Luo, B. Li, C. Zhang, Portable device for acetone detection based on cataluminescence sensor utilizing wireless communication technique, Sensor. Actuator. B Chem. 257 (2018) 451–459, https://doi.org/10.1016/j.snb.2017.10.154.
[12] L.J. Wang, Y.C. Chang, R. Sun, L. Li, A multichannel smartphone optical biosensor for high-throughput point-of-care diagnostics, Biosens. Bioelectron. 87 (2017) 686–692, https://doi.org/10.1016/j.bios.2016.09.021.
[13] G. Comina, A. Suska, D. Filippini, Towards autonomous lab-on-a-chip devices for cell phone biosensing, Biosens. Bioelectron. 77 (2016) 1153–1167, https://doi.org/10.1016/j.bios.2015.10.092.
[14] O. Hosu, A. Ravalli, G.M. Lo Piccolo, C. Cristea, R. Sandulescu, G. Marrazza, Smartphone-based immunosensor for CA125 detection, Talanta 166 (2017) 234–240, https://doi.org/10.1016/j.talanta.2017.01.073.
[15] X. Wang, M.R. Gartia, J. Jiang, T.W. Chang, J. Qian, Y. Liu, X. Liu, G.L. Liu, Audio jack based miniaturized mobile phone electrochemical sensing platform, Sensor. Actuator. B Chem. 209 (2015) 677–685, https://doi.org/10.1016/j.snb.2014.12.017.
[16] Y. Zhang, J. Yang, J. Nie, J. Yang, D. Gao, L. Zhang, J. Li, Enhanced ELISA using a handheld pH meter and enzyme-coated microparticles for the portable, sensitive detection of proteins, Chem. Commun. 52 (2016) 3474–3477, https://doi.org/10.1039/c5cc09852a.
[17] D. Bueno, R. Muñoz, J.L. Marty, Fluorescence analyzer based on smartphone camera and wireless for detection of Ochratoxin A, Sensor. Actuator. B Chem. 232 (2016) 462–468, https://doi.org/10.1016/j.snb.2016.03.140.
[18] A. Roda, E. Michelini, M. Zangheri, M. Di Fusco, D. Calabria, P. Simoni, Smartphone-based biosensors: a critical review and perspectives, TrAC Trends Anal. Chem. (Reference Ed.) 79 (2016) 317–325, https://doi.org/10.1016/j.trac.2015.10.019.
[19] S. Kempahanumakkagari, K. Vellingiri, A. Deep, E.E. Kwon, N. Bolan, K.H. Kim, Metal–organic framework composites as electrocatalysts for electrochemical sensing applications, Coord. Chem. Rev. 357 (2018) 105–129, https://doi.org/10.1016/j.ccr.2017.11.028.
[20] F. Li, H. Li, Z. Wang, J. Wu, W. Wang, L. Zhou, Q. Xiao, Q. Pu, Mobile phone mediated point-of-care testing of HIV p24 antigen through plastic micro-pit array chips, Sensor. Actuator. B Chem. 271 (2018) 189–194, https://doi.org/10.1016/j.snb.2018.05.090.
[21] S.K. Vashist, T. van Oordt, E.M. Schneider, R. Zengerle, F. von Stetten, J.H.T. Luong, A smartphone-based colorimetric reader for bioanalytical applications using the screen-based bottom illumination provided by gadgets, Biosens. Bioelectron. 67 (2015) 248–255, https://doi.org/10.1016/j.bios.2014.08.027.
[22] D. Quesada-González, A. Merkoçi, Mobile phone-based biosensing: an emerging "diagnostic and communication" technology, Biosens. Bioelectron. 92 (2017) 549–562, https://doi.org/10.1016/j.bios.2016.10.062.
[23] S.K. Vashist, E. Marion Schneider, R. Zengerle, F. von Stetten, J.H.T. Luong, Graphene-based rapid and highly-sensitive immunoassay for C-reactive protein using a smartphone-based colorimetric reader, Biosens. Bioelectron. 66 (2015) 169–176, https://doi.org/10.1016/j.bios.2014.11.017.
[24] S. Vashist, E. Schneider, J. Luong, Commercial smartphone-based devices and smart applications for personalized healthcare monitoring and management, Diagnostics 4 (2014) 104–128, https://doi.org/10.3390/diagnostics4030104.
[25] Y. Liang, X. Huang, X. Chen, W. Zhang, G. Ping, Y. Xiong, Plasmonic ELISA for naked-eye detection of ochratoxin A based on the tyramine-H2O2 amplification system, Sensor. Actuator. B Chem. 259 (2018) 162–169, https://doi.org/10.1016/j.snb.2017.12.004.
[26] S. Menon, A.R. Jose, S. Jesny, K.G. Kumar, A colorimetric and fluorometric sensor for the determination of norepinephrine, Anal. Methods. 8 (2016) 5801–5805, https://doi.org/10.1039/C6AY01539E.
[27] J. Pla-Tolós, Y. Moliner-Martínez, C. Molins-Legua, P. Campíns-Falcó, Solid glucose biosensor integrated in a multi-well microplate coupled to a camera-based detector: application to the multiple analysis of human serum samples, Sensor. Actuator. B Chem. 258 (2018) 331–341, https://doi.org/10.1016/j.snb.2017.11.069.
[28] R. Li, M. Zhen, M. Guan, D. Chen, G. Zhang, J. Ge, P. Gong, C. Wang, C. Shu, A novel glucose colorimetric sensor based on intrinsic peroxidase-like activity of C60-carboxyfullerenes, Biosens. Bioelectron. 47 (2013) 502–507, https://doi.org/10.1016/j.bios.2013.03.057.
[29] B. Ding, Y. Si, X. Wang, J. Yu, L. Feng, G. Sun, Label-free ultrasensitive colorimetric detection of copper(ii) ions utilizing polyaniline/polyamide-6 nano-fiber/net sensor strips, J. Mater. Chem. 21 (2011) 13345–13353, https://doi.org/10.1039/c1jm11851j.
[30] B.T.E. Thornton, A. Harrison, A.L. Pham, C.E. Castano, C. Tang, Polyaniline-functionalized nanofibers for colorimetric detection of HCl vapor, ACS Omega 3 (2018) 3587–3591, https://doi.org/10.1021/acsomega.8b00054.
[31] L. Kumar, I. Rawal, A. Kaur, S. Annapoorni, Flexible room temperature ammonia sensor based on polyaniline, Sensor. Actuator. B Chem. 240 (2017) 408–416, https://doi.org/10.1016/j.snb.2016.08.173.
[32] C. Thiemann, C.M.A. Brett, Electrosynthesis and properties of conducting polymers derived from aminobenzoic acids and from aminobenzoic acids and aniline, Synth. Met. 123 (2001) 1–9, https://doi.org/10.1016/S0379-6779(00)00364-7.
[33] A. Ravalli, C. Rossi, G. Marrazza, Bio-inspired fish robot based on chemical sensors, Sensor. Actuator. B Chem. 239 (2017) 325–329, https://doi.org/10.1016/j.snb.2016.08.030.
[34] C.C. Chen, Y. Gu, Enhancing the sensitivity and stability of HRP/PANI/Pt electrode by implanted bovine serum albumin, Biosens. Bioelectron. 23 (2008) 765–770, https://doi.org/10.1016/j.bios.2007.08.014.
[35] D.I. Torres, M.V. Miranda, V. Campo Dall' Orto, One-pot preparation of SBP-PANI-PAA-ethylene glycol diglycidyl ether sensor for electrochemical detection of H2O2, Sensor. Actuator. B Chem. 239 (2017) 1016–1025, https://doi.org/10.1016/j.snb.2016.08.110.
[36] L.R. Nemzer, A.J. Epstein, A polyaniline-based optical biosensing platform using an entrapped oxidoreductase enzyme, Sensor. Actuator. B Chem. 150 (2010) 376–383, https://doi.org/10.1016/j.snb.2010.06.054.
[37] G. Selvolini, I. Băjan, O. Hosu, C. Cristea, R. Săndulescu, G. Marrazza, DNA-based sensor for the detection of an organophosphorus pesticide: Profenofos, Sensors (2018) 18, https://doi.org/10.3390/s18072035.
[38] T. Homma, M. Kondo, T. Kuwahara, M. Shimomura, Polyaniline/poly(acrylic acid) composite film: a promising material for enzyme-aided electrochemical sensors, Eur. Polym. J. 62 (2015) 139–144, https://doi.org/10.1016/j.eurpolymj.2014.11.017.
[39] J. Lai, Y. Yi, P. Zhu, J. Shen, K. Wu, L. Zhang, J. Liu, Polyaniline-based glucose biosensor: a review, J. Electroanal. Chem. 782 (2016) 138–153, https://doi.org/10.1016/j.jelechem.2016.10.033.
[40] M. Porcel-Valenzuela, J. Ballesta-Claver, I. De Orbe-Payá, F. Montilla, L.F. Capitan-Vallvey, Disposable electrochromic polyaniline sensor based on a redox response using a conventional camera: a first approach to handheld analysis, J. Electroanal. Chem. 738 (2015) 162–169, https://doi.org/10.1016/j.jelechem.2014.12.002.
[41] A. Amine, G.J. Patriarche, G. Marrazza, M. Mascini, Amperometric determination of glucose in undiluted food samples, Anal. Chim. Acta 242 (1991) 91–98, https://doi.org/10.1016/0003-2670(91)87051-8.
[42] P. Bollella, L. Gorton, Enzyme based amperometric biosensors, Curr. Opin. Electrochem. 10 (2018) 157–173, https://doi.org/10.1016/j.coelec.2018.06.003.
[43] A. Ravalli, L. Lozzi, G. Marrazza, Micro-flow immunosensor based on thin-film interdigitated gold array microelectrodes for cancer biomarker detection, Curr. Drug Deliv. 13 (2016) 400–408, https://doi.org/10.2174/1567201812666151029101217.
[44] R.-S. Saberi, S. Shahrokhian, G. Marrazza, Amplified electrochemical DNA sensor based on polyaniline film and gold nanoparticles, Electroanalysis 25 (2013) 1373–1380, https://doi.org/10.1002/elan.201200434.
[45] O. Hosu, K. Elouarzaki, K. Gorgy, C. Cristea, R. Sandulescu, R.S. Marks, S. Cosnier, Nanostructured photoactivatable electrode surface based on pyrene diazirine, Electrochem. Commun. 80 (2017) 5–8, https://doi.org/10.1016/j.elecom.2017.05.002.
[46] M.D. Fairchild, Color Appearance Models, John Wiley & Sons, Chichester, England, 2013.
[47] F. Ahmad Rafiqi, K. Majid, Removal of copper from aqueous solution using polyaniline and polyaniline/ferricyanide composite, J. Environ. Chem. Eng. 3 (2015) 2492–2501, https://doi.org/10.1016/j.jece.2015.09.013.
[48] M.E. Mahmoud, E.A. Saad, A.M. El-Khatib, M.A. Soliman, E.A. Allam, N.A. Fekry, Green solid synthesis of polyaniline-silver oxide nanocomposite for the adsorptive removal of ionic divalent species of Zn/Co and their radioactive isotopes 65Zn/60Co, Environ. Sci. Pollut. Res. 25 (2018) 22120–22135, https://doi.org/10.1007/s11356-018-2284-8.
[49] C.M.A. Brett, A.M.O. Brett, Electroanalysis, Oxford University Press, 1998.
[50] I.Y. Sapurina, M.A. Shishov, Oxidative polymerization of aniline: molecular synthesis of polyaniline and the formation of supramolecular structures, in: A.D.S. Gomes (Ed.), New Polym. Spec. Appl. InTech, London, 2012, pp. 251–313 https://doi.org/10.5772/57353.
[51] Y. Si, X. Wang, Y. Li, K. Chen, J. Wang, J. Yu, H. Wang, B. Ding, Optimized colorimetric sensor strip for mercury(II) assay using hierarchical nanostructured conjugated polymers, J. Mater. Chem. A. 2 (2014) 645–652, https://doi.org/10.1039/c3ta13867d.